Multipath Effects in Ultrawideband Rake Reception

Wasim Q. Malik, *Member, IEEE*, Christopher J. Stevens, and David J. Edwards

***Abstract*—Rake reception can improve system performance significantly in wideband multipath channels. Its practical implementation, however, becomes prohibitively expensive in channels with dense multipath, such as the ultrawideband (UWB) channel. This paper investigates the effect of various system and environment parameters on rake performance, with emphasis on the amount of multipath and channel bandwidth. The treatment includes hybrid selection/maximal-ratio combining (H-S/MRC) and unordered, partial combining rake architectures, and is based on indoor channel measurements in the FCC-allocated UWB frequency range (3.1–10.6 GHz). The diversity gain is shown to follow the law of diminishing returns with the rake complexity. It is demonstrated that the rake can extract most of the incident signal power by combining only a subset of the resolved multipath components. The required number of rake fingers increases linearly with the number of resolved paths but sublinearly with the channel bandwidth. The characterization of the interplay of bandwidth, amount of scattering and rake complexity will facilitate efficient implementation of UWB systems.**

***Index Terms*—Diversity combining, hybrid selection/maximal-ratio combining (H-S/MRC), indoor propagation, multipath fading, rake receiver, ultrawideband (UWB).**

I. Introduction

INDOOR wireless communications channels typically experience significant multipath propagation [1]. A conventional narrowband system lacks the temporal resolution required to separate the closely arriving paths and detects the combined envelope as a single faded signal. Multipath resolution, however, increases as the bandwidth increases. An ultrawideband (UWB) system is therefore capable of resolving individual multipath arrivals with pathlength differences on the order of centimeters [2]. Consequently, a UWB system is less prone to multipath fading, with a significantly reduced small-scale fade range. Furthermore, UWB can exploit the multipath with rake combining [3] to boost the post-detection signal-to-noise ratio (SNR) at the receiver with the same transmit power, reducing the probability of outage. As UWB signals must obey the regulatory limits on power emission [2], this reception scheme can improve the link quality and extend its range [4].

Manuscript received May 28, 2006; revised August 19, 2007. This work was supported in part by the U.K. Engineering and Physical Sciences Research Council via Grant GR/T21769/01 and in part by the ESU Lindemann Trust.

W. Q. Malik is with the Laboratory for Information and Decision Systems, Massachusetts Institute of Technology, Cambridge, MA 02139 USA (e-mail: wqm@mit.edu).

C. J. Stevens and D. J. Edwards are with the Department of Engineering Science, University of Oxford, Oxford OX1 3PJ, U.K. (e-mail: christopher.stevens@eng.ox.ac.uk; david.edwards @eng.ox.ac.uk).

Color versions of one or more of the figures in this paper are available online at http://ieeexplore.ieee.org.

Digital Object Identifier 10.1109/TAP.2007.915414

A rake receiver consists of multiple branches, or fingers, that track individual multipath components (MPCs). The MPCs generally have unequal average SNRs. The finger outputs are combined using linear or decision-oriented diversity combining schemes. Two popular examples of linear diversity combining are selection combining (SC) and maximal-ratio combining (MRC) [3]. The optimal MRC rake, that combines all resolved paths, offers the highest SNR gain. MRC emphasizes the paths with the highest SNR, maximizing the output SNR provided those paths fade independently. A full-band UWB system spanning a 7.5 GHz bandwidth and operating in a rich scattering environment can often resolve over a hundred incident paths [5]. An MRC rake with such a large number of fingers is, however, impracticable with the current device technology. Suboptimal rake reception with hybrid selection/maximal-ratio combining (H-S/MRC), sometimes also referred to as general selection combining (GSC) [6] or selective rake (SRake) [7], offers a flexible alternative as it allows a tradeoff between complexity and performance by combining only a subset of the resolved paths [8], [9].

There has been considerable research on wideband and ultrawideband rake reception in recent years. Computationally efficient path selection algorithms for minimum mean-square error (MMSE) rake were presented in [10]. The effect of the number of resolved paths and bandwidth on reduced-complexity rake symbol-error probability (SEP) was determined analytically in [7], [9], [11]. Semi-analytical evaluation of UWB rake performance was performed using a statistical tapped-delay-line channel model in [12] and with a sparse channel assumption in [13]. An optimal spreading bandwidth was shown to exist for a rake with a given complexity in Rayleigh and Nakagami-m fading channels in [14], [15]. The SNR improvement as a function of rake complexity was obtained from UWB channel measurements in [16].

Several other rake implementations, optimized for specific channel conditions, have been presented. Generalized rake combining with maximum likelihood (ML) [17], and optimum combining with MMSE [18] and eigencanceler [19] implementations were proposed to combat narrowband or multiuser interference in wideband channels. Noncoherent rake techniques were presented for spread-spectrum systems in [20], while [21] proposed a noncoherent receiver for unresolvable paths. A hybrid adaptive MMSE rake and multiuser receiver for UWB communications was proposed in [22]. A scheme to tackle inter-symbol interference alongside rake reception for UWB channels was presented in [23]. Suboptimal UWB rakes with square-law combining (SLC) and MRC were compared in [24]. The performance of a coherent rake was found to be similar to an adaptive differential detector in [25]. It was concluded in [26] that imperfect channel estimation does not incur an appreciable penalty on a coherent rake, and also that a

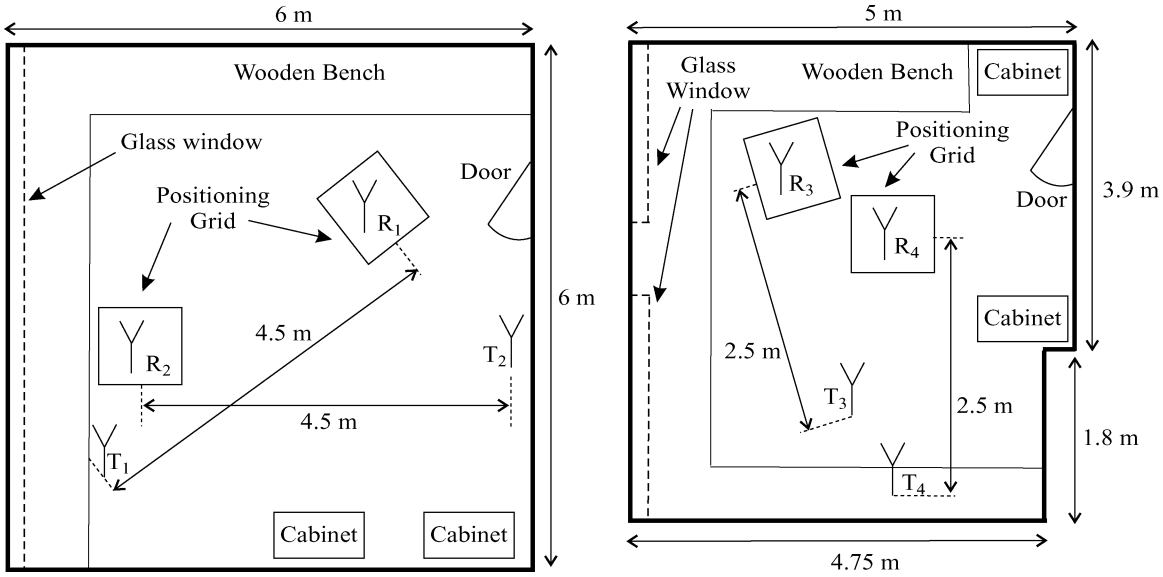

Fig. 1. Indoor propagation environment and measurement configuration. The measured links are defined by the $T_i R_i$ antenna pair, $i = \{1, \ldots, 4\}$.

fractionally-spaced rake outperforms a chip- or symbol-spaced rake. Antenna diversity was proposed as a means of reducing the required rake receiver complexity in [27] and [28].

This paper presents experimental results on the performance of optimal and suboptimal rake reception in indoor UWB channels. It provides a direct characterization of the relationship between the spreading bandwidth, number of resolved MPCs, rake complexity, diversity gain and bit-error probability. To our knowledge, the interplay of these parameters has not been investigated in detail. Following the nomenclature in [29], the diversity gain is defined in this paper in terms of the average improvement in received signal power, with the advantage that the results are independent of the signaling format. The analysis is based entirely on measured indoor line-of-sight (LOS) and non-line-of-sight (NLOS) channels, without relying on any theoretical channel models. Probabilistic representation is used to include the effect of channel-specific small-scale fading where required. A comparison of H-S/MRC (or selective rake) and PMRC (or partial rake) performance is made to determine the advantage of tracking some of the strongest paths, which has a bearing on receiver complexity. The variation in the rake output as a function of spreading bandwidth and number of resolved paths is assessed, and the optimal number of fingers required to capture a given percentage of the incident power is determined. The analysis culminates with semianalytical evaluation of the rake bit-error rate and its variation with the number of fingers and channel bandwidth. This comprehensive characterization offers valuable insight into rake receiver performance in real UWB channels, and provides simple and practical metrics for UWB communications system design.

II. Channel Measurements

Coherent channel measurements in the UWB band are performed in an indoor office environment, as shown in Fig. 1. A vector network analyzer (VNA), interfaced with a computer, is used for this purpose. The band between $f_l = 3.1$ GHz and $f_h = 10.6$ GHz (bandwidth $W = f_h - f_l = 7.5$ GHz) is sounded at $N_f = 1601$ discrete, equidistant frequency points, with frequency resolution $\Delta f = W/(N_f - 1) \approx 4.7$ MHz. Using low-loss RF cables, the VNA output port is connected to the transmitting antenna, and the input port to the receiving antenna through a wideband low-noise amplifier (LNA) with 30 dB gain. In this experiment, the channel is considered to be inclusive of the antennas. Therefore, the antennas are disconnected during end-to-end calibration of the equipment that removes frequency-dependent attenuation and phase distortion. The $S_{21}(f)$ complex transmission response of the channel is measured. The propagation environment consists of two small office rooms with block walls and several wooden and metallic objects. A number of reflective surfaces of various sizes are present, rendering the environment rich in multipath. Both LOS and NLOS scenarios are measured. The blockage for NLOS is created by placing a large block of RF-absorbant material vertically in the direct propagation path at a distance of 1 m from the transmitter, while the other aspects of the environment are kept identical to those in the LOS scenario. The physical space of the measurement is kept stationary throughout the duration of the experiment.

Two identical omnidirectional antennas, with discone construction and return loss well below -10 dB in the UWB band, are used to conduct the measurement [30]. The antennas are placed 1.5 m above the floor with their electric fields polarized vertically. Four sets of data are collected within the two rooms. In each measurement, the transmitting antenna is fixed at the point indicated in Fig. 1, while a computer-controlled planar positioning grid is used to position the receiving antenna at 900 individual points within a 1 mm^2 area, with 0.03 m spacing to allow sufficient decorrelation of the channel responses. The distance between the transmitting antenna and the center of the grid is 4.5 m in one room and 2.5 m in the other. In this manner, a total of 3600 LOS channel realizations and an equal number of NLOS realizations are obtained.

A single realization of the measured complex channel transfer function can be represented by

$$G(f) = \sum_{k=0}^{N_f-1} \alpha_k e^{j\phi_k} \delta(f - k\Delta f) \tag{1}$$

where α_k and ϕ_k are the magnitude and phase responses at the kth frequency component. The corresponding complex impulse response (CIR) of the channel is related to the transfer function through the Fourier transform, and can be expressed using a tapped delay line representation as

$$g(\tau) = \mathcal{F}^{-1}\{G(f)\} = \sum_{n=0}^{T-1} A_n e^{j\theta_n} \delta(\tau - n\Delta\tau) \tag{2}$$

where A_n and θ_n are the magnitude and phase responses in the kth time-bin, $\Delta\tau = 1/W$ is the time resolution, and T is the number of resolvable timebins in the CIR. The variable τ represents the time delay with reference to the time-of-arrival of the first MPC. The CIR is then power-normalized with respect to its norm to remove signal attenuation due to large and small scale fading, which is not relevant here, to obtain

$$\begin{aligned} h(\tau) &= \frac{g(\tau)}{\sqrt{\sum_{n=0}^{T-1} A_n^2}} = \sum_{n=0}^{T-1} a_n e^{j\theta_n} \delta(\tau - n\Delta\tau) \\ &= \sum_{l=1}^{N} a_l e^{j\theta_l} \delta(\tau - \tau_l) \end{aligned} \tag{3}$$

where N is the number of resolved MPCs, and a_l, θ_l and τ_l represent the magnitude, phase and time delay of the lth MPC.

From the inspection of individual CIRs obtained from our measurements, it is found that the received signal reaches a constant level at approximately 30 dB below the amplitude of the strongest path, and no significant multipath arrivals can be detected beyond this point. Thus, to remove the noise with an adequate margin, a 20 dB threshold is used with respect to the strongest signal in the CIR. After removing the noise and residual signal that falls below the threshold, the MPCs are identified by local maxima detection across the time-bins. The magnitude, phase and delay information of the individual MPCs in each CIR within the measurement ensemble is used for subsequent rake performance analysis.

III. Rake Receiver Model

When a UWB signal waveform, $s(t)$, propagates through a frequency-selective channel, $h(\tau)$, the signal

$$r_{\text{in}}(t) = \sqrt{E_s} s(t) * h(\tau) + n(t) \tag{4}$$

reaches the receiver, where $n(t) \sim \mathcal{CN}(0, N_0)$ is the additive white Gaussian noise. A rake receiver with linear diversity combining, shown in Fig. 2, integrates the power from the resolved

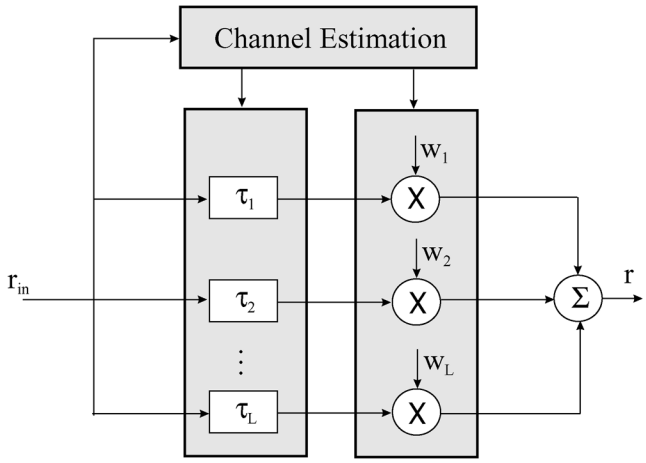

Fig. 2. A coherent rake receiver with L fingers and finger weight vector $\mathbf{w} = [w_1, \ldots, w_L]$.

paths by appropriately weighting and combining the co-phased copies of the received signal in each of its L fingers [3]. In the general form, its output can be represented by

$$r = \sum_{l=1}^{L} w_l a_l, \quad 1 \le L \le N \tag{5}$$

where w_l is the weighting factor for the lth finger, a_l is the magnitude of the corresponding path, and N is the number of incident MPCs. Under the constraint $\sum_{l=1}^{L} w_l = 1$, we have $w_l = 1/L$ for equal gain combining (EGC), while for maximal-ratio combining (MRC), $w_l \propto a_l$. In this paper, we will only consider MRC rake systems, as they provide the upper bound on linear-combining rake performance. The MPC SNRs are represented by $\{\gamma_1, \ldots, \gamma_N\}$. In the selective rake configuration, the paths are ordered on the basis of SNR prior to combining, given by $\{\gamma_{(1)}, \ldots, \gamma_{(N)}\}$, where $\gamma_{(1)} \ge \ldots \ge \gamma_{(N)}$. We consider the following rake configurations.

A. Maximal-Ratio Combining

In this paper, we refer to an ideal rake receiver, or the all-rake, simply as an MRC rake. Such a rake can, by definition, combine all of the incident paths and therefore possesses sufficient fingers. With weighting factors $w_i \propto a_i$, it yields a signal with output SNR given by

$$\gamma_{\text{MRC}} = \sum_{l=1}^{L} \gamma_l = \sum_{l=1}^{N} \gamma_l, \quad L \ge N. \tag{6}$$

B. Selection Combining

An SC rake has only one finger, i.e. $L = 1$. It processes all N resolved paths and selects the one with the highest SNR, such that its output SNR is

$$\gamma_{\text{SC}} = \gamma_{(1)}. \tag{7}$$

C. Hybrid-Selection/Maximal-Ratio Combining

Combining a large number of MPCs can result in an unnecessarily complex receiver. The complexity arises from the estimation of the channel parameters, *viz*. the multipath delays and gains, not known *a priori* in a realistic fading channel [36]. A reduced-complexity L-finger rake configuration uses H-S/MRC to combine the L strongest paths after weighting them according to their SNRs. The rake output SNR is then

$$\gamma_{\mathrm{H-S/MRC}} = \sum_{l=1}^{L} \gamma_{(l)}, \quad 1 \le L \le N. \tag{8}$$

D. Partial Maximal-Ratio Combining

Another suboptimal combining scheme with lower complexity than H-S/MRC is partial combining or PMRC. It also uses weighted path integration, similar to MRC, but does not order the paths according to their SNRs, reducing the channel estimation complexity associated with detecting and tracking the strongest L paths. Its output SNR is given by

$$\gamma_{\mathrm{PMRC}} = \sum_{l=1}^{L} \gamma_l, \quad 1 \le L \le N. \tag{9}$$

The relative magnitudes of the MPCs, a_l, determine the amount of additional power that can be captured from them. Also, the multipath fading correlation determines the achievable multipath diversity gain and fade mitigation, as is well-known from the perspective of diversity combining system performance in correlated fading channels [31]. If the noise is uniform across all the MPCs, as can be reasonably expected, the comparative analysis of path power can instead be treated in terms of the path SNRs. The receiver SNR influences the probability of outage, bit-error rate, and channel capacity.

IV. Rake Performance Analysis

In this section, we investigate in detail the performance of a UWB rake system. Our analysis is based on the achievable multipath diversity gain and bit-error rate (BER) improvement.

A. Diversity Gain

In order to assess the PMRC and H-S/MRC rake performance, we define the rake diversity gain as the ratio of the rake output SNR to the SNR of an arbitrarily chosen single MPC. The latter is taken in this analysis as the first arriving MPC, after noise and propagation delay removal, so that the rake diversity gain can be given by

$$\Delta\gamma = \gamma_{\mathrm{rake}}/\gamma_1 \tag{10}$$

where γ_{rake} for a given rake configuration is defined according to Section III. This is consistent with [29], where the diversity gain is defined as the increase in the received power due to the diversity system, which corresponds to SNR gain when the noise is uncorrelated and zero-mean Gaussian distributed.

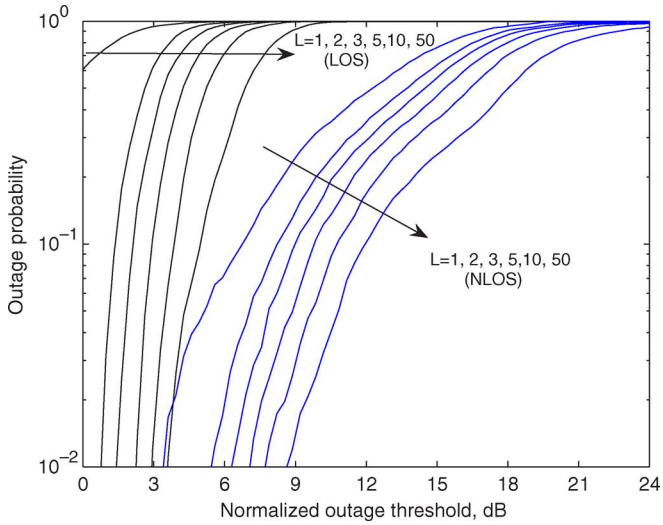

Fig. 3. The diversity gain of the L-finger H-S/MRC rake.

PMRC and H-S/MRC rake reception is applied individually to each CIR in the measurement ensemble to calculate the diversity gain. Note that if $L > N$, we extend (6)–(9) to assign $\gamma_k = 0 \; \forall \; N < k \le L$. The statistics of $\Delta\gamma$, such as its cumulative distribution function (CDF), $P(\Delta\gamma)$, are estimated over this ensemble. Fig. 3 shows $P(\Delta\gamma)$ of the H-S/MRC rake for some selected values of the number of fingers, L. An increase in L leads to an increase in the rake output SNR and consequently the diversity gain, but the fractional gain per finger diminishes at large L. At 1% outage probability, the difference between $L = 1$ and $L = 2$ for the H-S/MRC rake is 1 dB in LOS and 2 dB in NLOS. Fig. 3 also suggests that the diversity gain variance decreases with L, and the CDFs become steeper in general. The reason for this reduced variance is the increased multipath diversity at large L and the consequent averaging of the set of independent fading processes at each finger.

We now evaluate the mean and standard deviation of $\Delta\gamma$. Also of practical interest is the outage diversity gain, usually considered at 1% outage or 99% system reliability [29]. All of these quantities are plotted in Fig. 4 as functions of L. A comparison of H-S/MRC and PMRC rakes allows an evaluation of the benefit from path selection on the basis of SNR. It is observed that an SC rake (H-S/MRC rake with $L = 1$) provides 1 dB SNR gain in the LOS channel and 12 dB in the NLOS channel on average. At 1% outage, these values are 0.8 dB and 3.5 dB respectively. As the SNR of the PMRC rake with $L = 1$ is the reference point, for this rake we have $\Delta\gamma = 0$. An increase in L is accompanied by a sharp increase in $\Delta\gamma$ for the H-S/MRC rake, but the fractional gain saturates as L increases. The decline in the fractional gain is well known for diversity combining systems, due to which suboptimal implementations find favor in practical systems. From the figure, the diversity gain of an H-S/MRC rake at 1% outage is 4 dB in LOS and 9 dB in NLOS asymptotically in large L. We emphasize that the precise values depend on the measurement environment, CIR noise threshold, and other factors. It can be observed that $\Delta\gamma_{\mathrm{PMRC}} \to \Delta\gamma_{\mathrm{H-S/MRC}}$ as $L \to \infty$. From these results, we

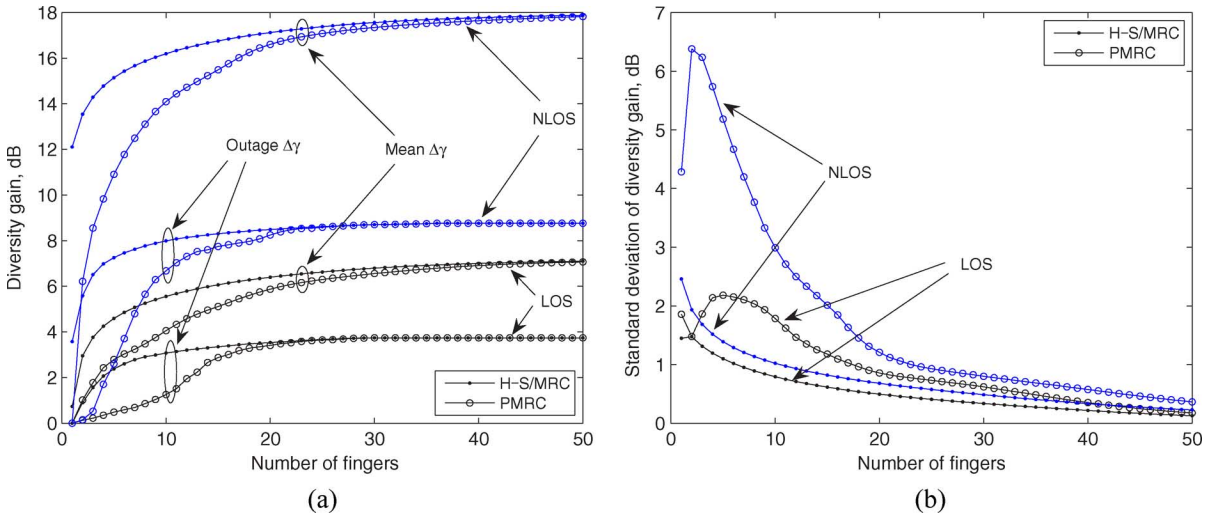

Fig. 4. Statistics of the diversity gain, $\Delta\gamma$, of H-S/MRC and PMRC rake receivers as a function of the number of fingers, L. (a) At the mean and 1% outage levels and (b) standard deviation.

can infer that a selective rake with realistic complexity offers substantially higher performance than a partial rake, but at the cost of the complexity associated with real-time path selection. Environments with temporally clustered multipath [32] can thus severely degrade the performance of a low-order PMRC rake, as the energy of the late-arriving strong MPCs is not captured with such a receiver. Its performance, therefore, is strongly dependent on the scattering environment and the extent of multipath propagation. Our results extend the previously reported conclusions drawn analytically for wideband Gaussian and Rayleigh fading channels [9], [33].

Fig. 4(b) shows that the standard deviation of $\Delta\gamma$ for H-S/MRC decreases monotonically in L, while that for PMRC has a peak in the region $2 \leq L \leq 5$. The latter is due to the relative stability of the direct path power (captured by the first finger, $L = 1$) but power variation in the following MPCs. In each case, the standard deviation approaches 0 asymptotically in L, i.e., $\Delta\gamma$ converges to a deterministic value as $L \to \infty$.

B. Dependence on Bandwidth

So far we have evaluated the rake performance over the entirety of the FCC UWB band (3.1–10.6 GHz). The effect of bandwidth variation is investigated next. To this end, spectral sections from the measured channel data are used to generate subchannels with reduced bandwidth $W_b < W$, similar to the approach in [34]. For fair comparison, the center frequency, f_c, and the number of frequency points, N_f, are kept constant, and $\Delta\tau$ is also constant. If N_b represents the number of resolved MPCs at W_b, then in general, $N_b \leq N$ when $W_b \leq W$, as bandwidth reduction lowers the multipath resolution. Consequently, multipath fading increases as W_b is reduced [34], and rake performance is also directly affected. A comprehensive analysis of the interplay between W_b, N_b, L, and $\Delta\gamma$ for the H-S/MRC rake follows in this section.

For a given channel with bandwidth W_b, the diversity gain is calculated using (10). Fig. 5 shows the variation of the 1% outage diversity gain with W_b for various values of L. Surprisingly, $\Delta\gamma$ is not a monotonic function of W_b. For a narrowband (single-tap) channel, $\Delta\gamma$ does not vary appreciably with L since an increase in the number of fingers cannot capture much additional power on account of the lack of multipath resolution. In a multipath channel, N_b increases with W_b, and therefore an H-S/MRC rake with $L > 1$ provides better performance than an SC rake in the wideband channel. However, as W_b increases further, $\Delta\gamma$ starts to decrease after reaching its peak at some bandwidth W_0. Physically, N_b increases with W_b when $0 \leq W_b \leq W_0$; at W_0, most of the incident multipath has been resolved, and a further increase in W_b yields a much reduced increase in N_b. On the other hand, as W_b increases, the channel energy gets distributed among a larger number of taps. A single rake finger, with capture time $\Delta\tau$, cannot therefore capture all of the dispersed energy. The consequence is that as W_b increases, the energy captured by a suboptimal rake with a given number of fingers decreases. This behavior is indicated by the negative slope of $\Delta\gamma/W_b$ in Fig. 5. Similar behavior is observed in the NLOS channel. This result, and its physical reasoning, agrees with and extends the earlier observation of an optimal spreading bandwidth that minimizes the bit-error rate [15].

In view of this relationship, we can expect that there is an optimal bandwidth W_b, corresponding to a given L_b, which offers the best rake complexity—power capture tradeoff. To investigate this, the number of H-S/MRC rake fingers, $L_{X\%}$, required to capture $X\%$ of the incident power is calculated and its relationship with W_b is investigated for $X = 99, 90, 50$ in Fig. 6. It can be observed that $L_{X\%}$, like $\Delta\gamma$, is a nonlinear function of W_b, reaching its peak at a certain bandwidth, after which it saturates. From the figure, a rake with 10 fingers can capture half of the incident power at any bandwidth, but larger L is required for larger X. For a rake with given complexity, there appears to be no gain from increasing the bandwidth beyond a certain optimal bandwidth, as the more dominant of the incident MPCs are already substantially resolved. For a given W_b, the variance of $L_{X\%}$ over the channel ensemble is larger in NLOS than in LOS, and also increases with X.

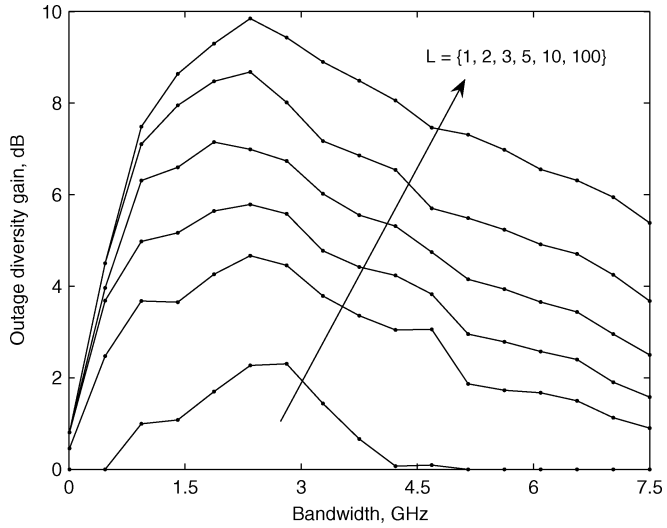

Fig. 5. The 1% outage diversity gain of the L-finger H-S/MRC rake as a function of channel bandwidth in the LOS channel.

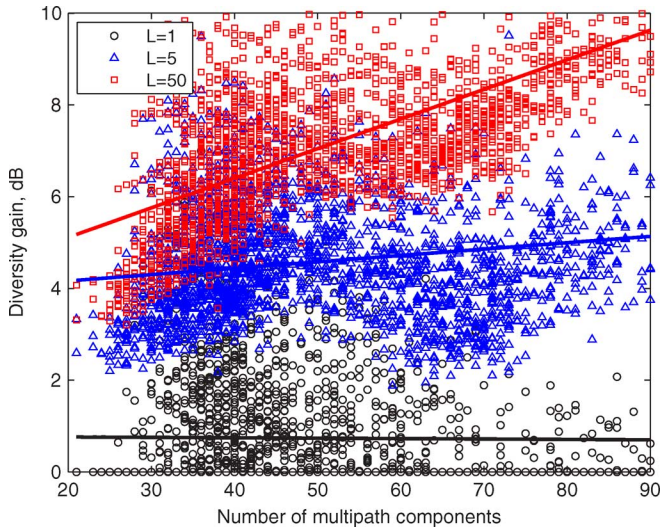

Fig. 7. Diversity gain of the L-finger H-S/MRC rake as a function of the number of paths at bandwidth $W = 7.5$ GHZ in the LOS channel.

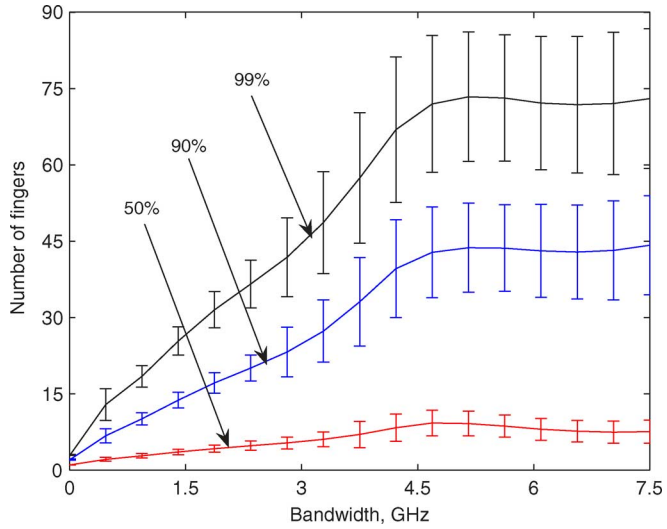

Fig. 6. Number of H-S/MRC rake fingers, $L_{X\%}$, required to capture $X\%$ of the incident power in the LOS channel. The solid lines and error bars represent the mean and standard deviation of $L_{X\%}$.

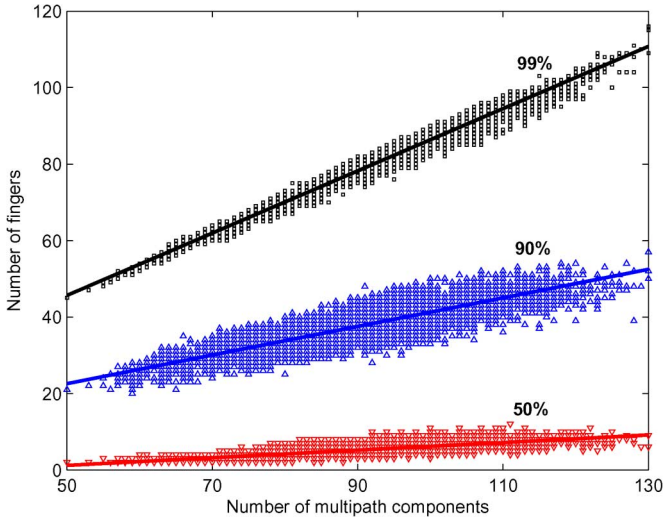

Fig. 8. Number of H-S/MRC rake fingers required to capture the specified percentage of the incident multipath power at bandwidth $W = 7.5$ GHz in the LOS channel.

C. Dependence on Number of Paths

Next, the relationship between N, L and $\Delta\gamma$ is evaluated while keeping the bandwidth constant at 7.5 GHz. For this purpose, the number of MPCs in each CIR in the measurement ensemble is detected, and the diversity gain of the rake is evaluated. Fig. 7 shows the variation of $\Delta\gamma$ with N for some representative values of L, where the scatter points signify the observed values and the solid lines show the best-fit linear regression. As the number of resolvable MPCs in the CIR increases, $\Delta\gamma$ also generally increases. It is observed that $\Delta\gamma$ is not affected by N for the SC rake, while for more complex rakes, $\Delta\gamma/N$ has a positive slope that also increases with L. Thus we conclude that the diversity gain increases with the amount of scattering in the channel if the rake is complex enough to capitalize on the increased multipath.

This now leads us to the characterization of L, as a function of N, required to capture $X\%$ of the multipath power. From Fig. 8, $L_{X\%}$ has a linear relationship with N. The positive regression provides an approximate figure for the percentage of resolved paths that must be combined. Thus, from our measurement data, 10%, 45% or 90% of the resolved paths must be combined if it is desired to capture 50%, 90% or 99% of the power, respectively, in the LOS channel, while the NLOS channel requires slightly greater rake complexity.

D. Error Rate Improvement

It has been established in this paper that significant SNR enhancement is obtained at the detector as a result of rake reception. As BER is a monotonically decreasing function of SNR, rake reception improves the BER by means of its diversity gain. We now evaluate the error performance of the H-S/MRC rake using the semianalytical approach with measured channels. The system BER can be obtained by averaging the BER conditioned on the received instantaneous SNR per bit at the rake output,

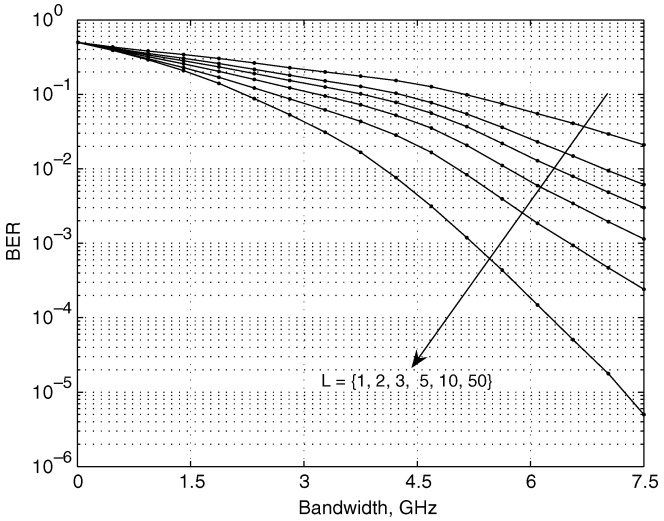

Fig. 9. Error performance of the L-finger H-S/MRC rake at 10 dB SNR in the LOS channel.

$\gamma_{\text{rake}}(x)$, over the probability density function (PDF), $p_{\gamma_{\text{rake}}}(x)$, of γ_{rake}, for the xth realization, i.e.,

$$P_e = \int_0^\infty P_e|_{\gamma_{\text{rake}}}(x) p_{\gamma_{\text{rake}}}(x) \mathrm{d}x. \tag{11}$$

Assuming binary antipodal modulation, we have [35]

$$P_e|_{\gamma_{\text{rake}}}(x) = \mathrm{Q}\left(\sqrt{2\rho\gamma_{\text{rake}}(x)}\right) \tag{12}$$

where Q(.) is the Marcum Q function, $\rho = E_s/N_0$ is the symbol SNR, and $\gamma_{\text{rake}}(x)$ is the instantaneous output SNR of the L-finger H-S/MRC rake normalized with respect to $\gamma_{\text{MRC}}(x)$. Fig. 9 shows the rake BER performance for various W_b and L_b, where $\rho = 10$ dB, and $\gamma_{\text{rake}}(x)$ is normalized to $\gamma_{\text{MRC}}(x)|_{W_b=7.5\text{ GHz}}$ to compare the trends. At large W_b, an increase in L_b leads to an BER improvement due to greater capture of the incident multipath power distributed among the channel taps. An increase in L_b from 1 to 5 reduces the BER by an order of magnitude when $W_b = 7.5$ GHz. The BER performance of the L_b-finger rake improves as the bandwidth increases, for reasons explained earlier in the paper.

V. Conclusion

This paper has analyzed the impact of the multipath propagation environment on the performance of a UWB rake receiver. The SNR improvement due to optimal and suboptimal rake receivers has been studied in measured UWB channels. The incremental rake improvement is found to fall rapidly with an increase in the number of fingers, validating earlier theoretical predictions based on simple channel models. The diversity gain of unordered, or partial, combining asymptotically approaches that of selective rake combining, but the performance difference is large with realistic complexity especially in NLOS channels. As the bandwidth, W_b, increases, the outage diversity gain of the H-S/MRC rake also increases first, reaching its peak and then diminishing, indicating that a certain optimal bandwidth is associated with a rake operating in a given environment. As W_b increases, the required number of fingers, L, increases to a certain point and then becomes constant. From the measurements, to capture 90% of the incident multipath-dispersed power in the UWB channel, about 5 fingers are sufficient at $W_b = 500$ MHz, but over 40 fingers are required beyond 4 GHz. The diversity gain increases linearly with the number of MPCs, N, and the slope increases with L. A linear relationship is also observed between the incident N and the L required to capture a given percentage of the power. From the experimental analysis in this paper, combining 45% of the paths yields 90% of the incident power at $W_b = 7.5$ GHz. The bit-error rate results show that the system performance improves from using a higher-order rake at large bandwidth. The analysis in this paper has provided practical metrics for the design of UWB systems that can be easily tailored to a given set of channel conditions and performance requirements.

References

[1] H. Hashemi, "The indoor radio propagation channel," *Proc. IEEE*, vol. 81, no. 7, pp. 943–968, Jul. 1993.

[2] B. Allen, M. Dohler, E. E. Okon, W. Q. Malik, A. K. Brown, and D. J. Edwards, Eds., *Ultra-Wideband Antennas and Propagation for Communications, Radar and Imaging*. London, U.K.: Wiley, 2006.

[3] G. L. Stüber, *Principles of Mobile Communications*, 2nd ed. Norwell, MA: Kluwer, 2001.

[4] S. Gaur and A. Annamalai, "Improving the range of ultrawideband transmission using rake receivers," in *Proc. IEEE Veh. Technol. Conf. (VTC)*, Orlando, FL, Oct. 2003, pp. 597–601.

[5] A. F. Molisch, "Ultrawideband propagation channels—Theory, measurement, and modeling," *IEEE Trans. Veh. Technol.*, vol. 54, no. 5, pp. 1528–1545, Sep. 2005.

[6] T. Eng, N. Kong, and L. B. Milstein, "Comparison of diversity combining techniques for Rayleigh fading channels," *IEEE Trans. Commun.*, vol. 44, no. 9, pp. 1117–1129, Sep. 1996.

[7] M. Z. Win and Z. A. Kostic, "Impact of spreading bandwidth on Rake reception in dense multipath channels," *IEEE J. Select. Areas Commun.*, vol. 17, no. 10, pp. 1794–1806, Oct. 1999.

[8] N. Kong and L. B. Milstein, "Combined average SNR of a generalized diversity selection combining scheme," in *Proc. IEEE Int. Conf. Commun. (ICC)*, Atlanta, GA, Jun. 7–11, 1998, pp. 1556–1560.

[9] M. Z. Win, G. Chrisikos, and N. R. Sollenberger, "Performance of Rake reception in dense multipath channels: Implications of spreading bandwidth and selection diversity order," *IEEE J. Select. Areas Commun.*, vol. 18, no. 8, pp. 1516–1525, Aug. 2000.

[10] S. Gezici, M. Chiang, H. V. Poor, and H. Kobayashi, "Optimal and suboptimal finger selection algorithms for MMSE rake receivers in impulse radio ultra-wideband systems," in *Proc. IEEE Wireless Commun. Networking Conf. (WCNC)*, New Orleans, LA, Mar. 2005, pp. 861–866.

[11] R. Maffei, U. Manzoli, and M. L. Merani, "Rake reception with unequal power path signals," *IEEE Trans. Commun.*, vol. 52, no. 1, pp. 24–27, Jan. 2004.

[12] D. Cassioli, M. Z. Win, F. Vatalaro, and A. F. Molisch, "Performance of low-complexity Rake reception in a realistic UWB channel," in *Proc. IEEE Int. Conf. Commun. (ICC)*, New York, Apr. 2002, pp. 763–767.

[13] M. Z. Win and R. A. Scholtz, "On the energy capture of ultrawide bandwidth signals in dense multipath environments," *IEEE Commun. Lett.*, vol. 2, no. 9, pp. 245–247, Sep. 1998.

[14] W. C. Lau, M.-S. Alouini, and M. K. Simon, "Optimum spreading bandwidth for selective RAKE reception over Rayleigh fading channels," *IEEE J. Select. Areas Commun.*, vol. 19, no. 6, pp. 1080–1089, Jun. 2001.

[15] D. Cassioli, M. Z. Win, F. Vatalaro, and A. F. Molisch, "Effects of spreading bandwidth on the performance of UWB rake receivers," in *Proc. IEEE Int. Conf. Commun. (ICC)*, Anchorage, AK, May 2003, pp. 3545–3549.

[16] W. Q. Malik, D. J. Edwards, and C. J. Stevens, "Experimental evaluation of Rake receiver performance in a line-of-sight ultra-wideband channel," in *Proc. Joint IEEE Ultra-Wideband Syst. Tech. and Int. Workshop Ultra-Wideband Syst. (UWBST & IWUWBS)*, Kyoto, Japan, May 2004, pp. 217–220.
[17] G. E. Bottomley, T. Ottosson, and Y.-P. E. Wang, "A generalized Rake receiver for interference suppression," *IEEE J. Select. Areas Commun.*, vol. 18, no. 8, pp. 1536–1545, Aug. 2000.
[18] I. Bergel, E. Fishler, and H. Messer, "Narrow-band interference suppression in time-hopping impulse-radio systems," in *Proc. IEEE Conf. Ultra-Wideband Sys. Tech. (UWBST)*, Baltimore, MD, May 2002, pp. 303–307.
[19] H. Sheng, A. M. Haimovich, A. F. Molisch, and J. Zhang, "Optimum combining for time hopping impulse radio UWB rake receivers," in *Proc. IEEE Conf. Ultra-Wideband Syst. Tech. (UWBST)*, Reston, VA, Nov. 2003, pp. 224–228.
[20] W. H. Sheen and G. L. Stüber, "A noncoherent tracking loop with diversity and multipath interference cancellation for direct-sequence spread-spectrum systems," *IEEE Trans. Commun.*, vol. 46, no. 11, Nov. 1998.
[21] V. Aue and G. P. Fettweis, "A non-coherent tracking scheme for the RAKE receiver that can cope with unresolvable multipath," in *Proc. IEEE Int. Conf. Commun. (ICC)*, Vancouver, Canada, Jun. 1999, pp. 1917–1921.
[22] Q. Li and L. A. Rusch, "Hybrid RAKE/multiuser receivers for UWB," in *Proc. IEEE Radio Wireless Conf.*, Boston, MA, Aug. 2003, pp. 203–206.
[23] A. G. Klein, D. R. Brown, D. L. Goeckel, and C. R. Johnson, "RAKE reception for UWB communication systems with intersymbol interference," in *Proc. IEEE Workshop Sig. Proc. Advances Wireless Commun. (SPAWC)*, Rome, Italy, Jun. 2003, pp. 244–248.
[24] J. D. Choi and W. E. Stark, "Performance of ultra-wideband communications with suboptimal receivers in multipath channels," *IEEE J. Select. Areas Commun.*, vol. 20, no. 9, pp. 1754–1766, Dec. 2002.
[25] G. Durisi and S. Benedetto, "Performance of coherent and non-coherent receivers for UWB communications," in *Proc. IEEE Int. Conf. Commun. (ICC)*, Paris, France, Jun. 2004, pp. 3429–3433.
[26] B. Mielczarek, M.-O. Wessman, and A. Svensson, "Performance of coherent UWB Rake receivers with channel estimators," in *Proc. IEEE Veh. Technol. Conf. (VTC)*, Orlando, FL, Oct. 2003, pp. 1880–1884.
[27] J. Keignart, C. Abou-Rjeily, C. Delaveaud, and N. Daniele, "UWB SIMO channel measurements and simulations," *IEEE Trans. Microwave Theory Tech.*, vol. 54, no. 4, pp. 1812–1819, Apr. 2006.
[28] W. Q. Malik and D. J. Edwards, "UWB impulse radio with triple-polarization SIMO," in *Proc. IEEE Global Commun. Conf. (Globecom)*, Washington, DC, Nov. 2007, pp. 4124–4128.
[29] D. G. Brennan, "Linear diversity combining techniques," *Proc. IRE*, vol. 47, pp. 331–356, Jun. 1959.
[30] W. Q. Malik, D. J. Edwards, and C. J. Stevens, "Angular-spectral antenna effects in ultra-wideband communications links," *Proc. Inst. Elect. Eng. Commun.*, vol. 153, no. 1, pp. 99–106, Feb. 2006.
[31] A. J. Paulraj, D. A. Gore, R. U. Nabar, and H. Bolcskei, "An overview of MIMO communications—A key to gigabit wireless," *Proc. IEEE*, vol. 92, no. 2, pp. 198–218, Feb. 2004.
[32] A. A. M. Saleh and R. A. Valenzuela, "A statistical model for indoor multipath propagation," *IEEE J. Select. Areas Commun.*, vol. SAC-5, no. 2, pp. 128–137, Feb. 1987.
[33] M. Z. Win and J. H. Winters, "Analysis of hybrid selection/maximal-ratio combining in Rayleigh fading," *IEEE Trans. Commun.*, vol. 47, no. 12, pp. 1773–1776, Dec. 1999.
[34] W. Q. Malik, B. Allen, and D. J. Edwards, "Fade depth scaling with channel bandwidth," *Electron. Lett.*, vol. 43, no. 24, pp. 1371–1372, Nov. 2007.
[35] J. G. Proakis, *Digital Communications*, 4th ed. New York: McGraw-Hill, 2001.

Wasim Q. Malik (M'05) received the B.E. degree from the National University of Sciences and Technology, Pakistan, in 2000 and the D.Phil. degree from the University of Oxford, Oxford, U.K., in 2005, both in electrical engineering.

From 2005 to 2007, he was a Research Fellow at the University of Oxford and a Junior Research Fellow in Science at Wolfson College, Oxford. Since 2007, he has been a Postdoctoral Fellow at the Massachusetts Institute of Technology, Cambridge. He is an editor of the book *Ultra-Wideband Antennas and Propagation for Communications, Radar and Imaging* (U.K.: Wiley, 2006), and was a Guest Editor of the *IET Microwaves Antennas and Propagation* Dec. 2007 Special Issue on Antenna Systems and Propagation for Future Wireless Communications. He has published in excess of 60 papers in refereed journals and conferences.

Dr. Malik received the ESU Lindemann Science Fellowship in 2007, the Best Paper Award in the ARMMS RF and Microwave Conf. (Steventon, U.K., April 2006), and the Association for Computing Machinery (ACM) Recognition of Service Award in 1997. He routinely serves on the organizing and technical program committees of various international conferences.

Christopher J. Stevens read physics at the University of Oxford, Oxford, U.K., graduating in 1990 with first class honors and prizes for practical physics and received the D.Phil. degree in condensed matter physics in 1994 following a three-year doctoral programme at the same university.

He has worked for the European Union Human Capital Mobility scheme at the Universita degli Studi di Lecce. Following this he moved back to Oxford for a three-year postdoctoral position on a program studying the physics of novel superconducting materials. In 1997, he obtained a Royal Academy of Engineering Senior Research Fellowship and moved disciplines to engineering. He now holds an engineering faculty position at the University of Oxford and is a Fellow of St. Hugh's College, Oxford. His current research activities include ultrawideband communications systems, applications of metamaterials, ultrafast nanoelectronics and high speed electromagnetics.

Dr. Stevens is a member of the Institution of Engineering and Technology (IET), London, U.K., and founder member of the VORTEX consortium.

David J. Edwards is a Professor of Engineering Science at the University of Oxford, Oxford, U.K. and a Fellow of Wadham College, Oxford. He has been an academic for 21 years after 12 years spent in the industry (British Telecom). He has a strong record of innovation in communications systems, techniques and technologies and has published in excess of 300 papers during his time as an academic. He has been awarded a number of patents and several have appeared as licensed commercial products. He has acted as a consultant to a large number of industrial organizations during his career, and has served on a number of national and international committees relating to antennas and propagation. Current research areas include electromagnetics, magneto-inductive waveguides, ultrawideband communications, ad hoc networks, and MIMO systems.

Prof. Edwards is a Fellow of the Institution of Engineering and Technology (IET), London, U.K., and the Royal Astronomical Society. He was the recipient of a number of awards and prizes for his work and has been extremely well supported by funding from research councils, industry, and government agencies.